Electronic supplementary information

New bimetallic palladium(II) and platinum(II) complexes: Studies of nucleophilic substitution reactions, interactions with CT-DNA, bovine serum albumin and cytotoxic activity

Snežana Jovanović[a], Katarina Obrenčević[b], Živadin D. Bugarčić[a], Iva Popović[c], Jelena Žakula [c] and Biljana Petrović[a*]

[a]Faculty of Science, University of Kragujevac, Domanovića 12, P. O. Box 60,
34000 Kragujevac, Serbia

[b]Military Medical Academy, Crnotravska 17, 11000 Belgrade, Serbia

[c]Institute of Nuclear Sciences ‘‘Vinča”, University of Belgrade, Mike Petrovića Alasa 12-14, 11001 Belgrade, Serbia

*Corresponding author: Prof. Dr. Biljana Petrović, Phone: +381(0)34300262,
Fax: +381(0)34335040, e-mail: biljanap@kg.ac.rs

DNA-binding studies

Calculation of DNA-binding constants

The intrinsic binding constant, K_b, was determined using the Eq. (S1)[1]:

$$[DNA]/(\varepsilon_A - \varepsilon_f) = [DNA]/(\varepsilon_b - \varepsilon_f) + 1/[K_b(\varepsilon_b - \varepsilon_f)] \quad \text{(Eq. S1)}$$

K_b is given by the ratio of slope to the *y* intercept in plots $[DNA]/(\varepsilon_A - \varepsilon_f)$ *versus* [DNA] (Fig. S24), where [DNA] is the concentration of DNA in base pairs, $\varepsilon_A = A_{obsd}/[complex]$, ε_f is the extinction coefficient for the unbound complex and ε_b is the extinction coefficient for the complex in the fully bound form.

Stern-Volmer equation for EB competitive studies

Stern-Volmer quenching constant, K_{sv}, was calculated from the slope of straight line obtained from Stern-Volmer Eq. (S2)[2]:

$$I_0/I = 1 + K_{sv}[Q] \quad \text{(Eq. S2)}$$

where I_0 and I are the emission intensities in the absence and in the presence of the quencher (complexes **(1)**, **(2)** and **(3)**, respectively), [Q] is the total concentration of quencher, K_{sv} is the quenching constant.

Stern-Volmer equation for BSA studies

Dynamic quenching constant, K_{sv}, and the quenching constant, k_q, were calculated using the Stern-Volmer equation, Eq. (S3)[2]:

$$I_0/I = 1+ k_q\tau_0[Q] = 1+ K_{sv}[Q] \quad \text{(Eq. S3)}$$

where I_0 = the initial tryptophan fluorescence intensity of BSA, I = the tryptophan fluorescence intensity of BSA after the addition of the quencher, k_q = the quenching rate constants of BSA, K_{sv} = the dynamic quenching constant, τ_0 = the average lifetime of BSA without the quencher, [Q] = the concentration of the quencher respectively, τ_0 fluorescence lifetime of tryptophan in BSA at around 10^{-8} s.

Scatchard equation

Association binding constant (*K*) and the number of binding sites per albumin (*n*), can be calculated using Scatchard equation, Eq. (S4)[3]:

$$(\Delta I/I_0)/[Q] = nK - K\Delta I/I_0 \quad \text{(Eq. S4)}$$

where *K* may be calculated from the slope in the Scatchard plots $(\Delta I/I_0)/[Q]$ *vs* $\Delta I/I_0$ and *n* is given by the ratio of *y* intercept to the slope.

References:

1 A. M. Pyle, J. P. Rehmann, R. Meshoyrer, C. V. Kumar, N. J. Turro and J. K. Barton, *J .Am. Chem. Soc*., 1989, **111**, 3051-3058.

2 R. Lakowicz and G.Weber, *Biochemistry*, 1973, **12**, 4161-4170.

3 S. Wu, W. Yuan, H. Wang, Q. Zhang, M. Liu and K. Yu, *J. Inorg. Biochem*., 2008, **102**, 2026-2034.

Table S1. Selected chemical shifts for the investigated ligands and products from the reactions of complexes **(1)** and **(2)** marked as (Pd) and (Pt).

Species	δ(H6/H6')	δ(CH_3)	δ(CH)	δ(CH_2)	δ(H5)	δ(H1')	δ(H8)	2H/2H' (pyrazine)	3H/3H' (pyrazine)
Tu									
(1), **(Pd)**	9.15								
(1), **(Pt)**	9.42							8.78	9.08
(2), **(Pd)**									
(2), **(Pt)**								8.78	9.10
L-Met		2.15							
(1), **(Pd)**	8.50	2.71						8.55	
(1), **(Pt)**	8.70	2.75							8.90
(2), **(Pd)**		2.71						8.55	
(2), **(Pt)**		2.75							8.95
L-Cys			4.00	3.08					
(1), **(Pd)**	9.08		4.10	3.32					
(1), **(Pt)**	9.60		4.17	3.40				8.78	9.00
(2), **(Pd)**			4.10	3.20					
(2), **(Pt)**			4.15	3.27				8.78	9.10
L-His					7.13				
(1), **(Pd)**	9.18				7.03				
(1), **(Pt)**	9.54				7.07			8.78	9.08
(2), **(Pd)**					7.03				
(2), **(Pt)**					7.07			8.78	9.10
5'-GMP						5.85	8.25		
(1), **(Pd)**	8.53					6.25		8.55	
(1), **(Pt)**	8.70					6.35			8.90
(2), **(Pd)**						6.23	8.27	8.55	
(2), **(Pt)**						6.35	8.35		8.95

Table S2. Peaks detected in the positive ion MALDI-TOF mass spectrum of the complexes **(1)** and **(2)**, respectively. Due to a high number of isotopes that Pt and Pd have, these signals actually represent a group of individual peaks.

Peak position *(m/z)*	*m/z range*	Peak assignment
Complex (1)		
297.45	*297.45-301.38*	$[PdCl(bipy)]^+$
386.52	*386.52-390.52*	$[PtCl(bipy)]^+$
507.72	*505.69-507.72*	$[Pt(bipy)_2]^+$
542.45	*539.71-544.70*	$[PtCl(bipy)_2]^+$
800.31	*798.85-801.81*	$\{[PdPtCl_2(bipy)_2(pz)]Cl\}^+$ *
864.31	*864.31-871.10*	$\{[PdPtCl_2(bipy)_2(pz)](ClO_4)\}^+$ *
Complex (2)		
315.52	*313.58-317.52*	$[Pt(en)_2]^+$
335.52	*335.52-340.51*	$[Pt(en)(pz)]^{\cdot+}$
376.51	*372.51-377.52*	$[PtCl(en)(pz)]^+$
607.65	*607.65-616.74*	$\{[PdPtCl_2(en)_2(pz)]Cl\}^+$*
671.65	*671.65-672.27*	$\{[PdPtCl_2(en)_2(pz)](ClO_4)\}^+$ *

*Indicates species detectable only with the assistance of matrix, 2,5-DHB

Table S3. Observed *pseudo*-first order rate constants as a function of ligand concentration and temperature for the substitution reactions of complex **(1)** in 25 mM Hepes buffer (pH = 7.2) with the addition of 40 mM NaCl.

Ligand	T [K]	λ [nm]	10^3 C_L [M]	k_{obsd1} [s^{-1}]	k_{obsd2} [s^{-1}]	10^3 k_{obsd3} [s^{-1}]	10^4 k_{obsd4} [s^{-1}]
Tu	288	310	1	22.71(6)[a]	2.20(6)	-	-
			2	56.10(5)	4.88(6)	-	-
			3	81.52(4)	7.25(5)	-	-
			4	102.41(6)	9.28(4)	-	-
			5	127.09(6)	11.72(6)	-	-
	298		1	32.33(5)	2.88(6)	3.00(2)	2.80(2)
			2	63.56(4)	5.89(5)	5.90(3)	5.30(2)
			3	94.40(5)	8.04(4)	8.10(3)	6.80(3)
			4	120.30(4)	11.45(5)	11.00(3)	10.00(2)
			5	160.30(6)	13.88(4)	14.00(2)	13.00(2)
	308		1	40.84(4)	3.27(6)	-	-
			2	68.87(5)	7.12(4)	-	-
			3	108.76(5)	10.12(4)	-	-
			4	138.98(5)	13.58(5)	-	-
			5	187.31(6)	16.94(6)	-	-
Ligand	T [K]	λ [nm]	10^3 C_L [M]	k_{obsd1} [s^{-1}]	10^3 k_{obsd2} [s^{-1}]		
L-Met	288	280	1	5.11(4)[a]	-	-	-
			2	9.21(5)	-	-	-
			3	15.71(5)	-	-	-
			4	19.94(4)	-	-	-
			5	24.19(6)	-	-	-
	298		1	7.57(5)	2.40(3)	-	-
			2	13.28(5)	4.40(2)	-	-
			3	20.14(4)	6.70(3)	-	-
			4	28.38(4)	9.10(3)	-	-
			5	34.49(6)	11.00(2)	-	-
	308		1	11.25(5)	-	-	-
			2	24.28(4)	-	-	-

			3	35.44(5)	-	-	-
			4	45.66(5)	-	-	-
			5	57.81(6)	-	-	-
Ligand	T [K]	λ [nm]	10^3 C_L [M]	k_{obsd1} [s^{-1}]	k_{obsd2} [s^{-1}]	10^3 k_{obsd3} [s^{-1}]	10^4 k_{obsd4} [s^{-1}]
L-Cys	288	280	1	4.78(5)	0.21(4)	-	-
			2	9.09(5)	0.36(5)	-	-
			3	13.24(6)	0.60(5)	-	-
			4	18.35(5)	0.71(5)	-	-
			5	22.68(6)	0.97(6)	-	-
	298		1	6.15(5)	0.32(4)	2.20(2)	1.30(2)
			2	11.59(5)	0.62(5)	4.00(2)	3.00(3)
			3	18.01(5)	0.93(5)	5.90(2)	4.00(2)
			4	24.01(6)	1.21(5)	7.80(3)	5.50(2)
			5	29.05(6)	1.54(5)	9.70(2)	6.90(3)
	308		1	8.79(4)	0.35(4)	-	-
			2	16.13(4)	0.67(5)	-	-
			3	24.96(5)	0.95(5)	-	-
			4	33.98(5)	1.30(5)	-	-
			5	41.41(6)	1.63(4)	-	-
Ligand	T [K]	λ [nm]	10^3 C_L [M]	k_{obsd1} [s^{-1}]	10^2 k_{obsd2} [s^{-1}]	10^3 k_{obsd3} [s^{-1}]	10^4 k_{obsd4} [s^{-1}]
L-His	288	280	1	2.45(4)	2.90(4)	-	-
			2	5.26(5)	5.30(5)	-	-
			3	7.28(4)	8.10(4)	-	-
			4	10.13(6)	11.00(5)	-	-
			5	12.37(5)	13.50(4)	-	-
	298		1	2.76(4)	6.90(4)	1.50(2)	1.18(2)
			2	6.44(5)	12.00(5)	3.30(2)	2.30(3)
			3	9.55(5)	20.00(5)	5.10(2)	3.50(2)
			4	12.51(4)	26.00(5)	6.80(3)	4.50(3)
			5	15.11(6)	32.00(5)	7.90(2)	5.80(3)
	308		1	4.20(4)	14.00(6)	-	-
			2	8.38(5)	25.00(5)	-	-
			3	12.93(5)	39.00(5)	-	-

			4	16.23(4)	51.00(5)	-	-
			5	20.56(4)	65.00(4)	-	-
Ligand	T [K]	λ [nm]	10^3 C_L [M]	k_{obsd1} [s^{-1}]	10^3k_{obsd2} [s^{-1}]		
5'-GMP	288	310	1	1.23(4)	-	-	-
			2	2.63(5)	-	-	-
			3	4.04(5)	-	-	-
			4	5.23(4)	-	-	-
			5	6.45(6)	-	-	-
	298		1	1.53(4)	0.77(3)	-	-
			2	2.98(5)	1.68(3)	-	-
			3	4.50(5)	2.50(2)	-	-
			4	6.05(5)	3.20(2)	-	-
			5	7.45(5)	4.05(3)	-	-
	308		1	2.14(4)	-	-	-
			2	4.45(5)	-	-	-
			3	6.30(5)	-	-	-
			4	8.33(5)	-	-	-
			5	10.86(4)	-	-	-

[a]Number of runs in parenthesis

Table S4. Observed *pseudo*-first order rate constants as a function of ligand concentration and temperature for the substitution reactions of complex **(2)** in 25 mM Hepes buffer (pH = 7.2) with the addition of 40 mM NaCl.

Ligand	T [K]	λ [nm]	10^3 C_L [M]	k_{obsd1} [s^{-1}]	k_{obsd2} [s^{-1}]	10^3 k_{obsd3} [s^{-1}]	10^4 k_{obsd4} [s^{-1}]
Tu	288	310	1	4.42(6)[a]	0.57(6)	-	-
			2	8.11(5)	0.98(6)	-	-
			3	12.64(4)	1.51(5)	-	-
			4	16.64(6)	2.09(4)	-	-
			5	21.09(6)	2.54(6)	-	-
	298		1	6.54(5)	0.78(6)	1.30(2)	2.22(2)
			2	11.31(5)	1.37(5)	2.53(3)	4.20(2)
			3	18.52(4)	2.12(4)	4.23(3)	5.91(3)
			4	23.79(4)	2.79(5)	5.20(3)	7.90(2)
			5	30.27(6)	3.60(4)	6.49(2)	10.50(2)
	308		1	10.45(4)	1.41(6)	-	-
			2	19.23(5)	2.87(4)	-	-
			3	29.12(5)	4.26(4)	-	-
			4	40.05(5)	5.68(5)	-	-
			5	48.81(6)	6.94(6)	-	-
Ligand	T [K]	λ [nm]	10^3 C_L [M]	k_{obsd1} [s^{-1}]	10^3 k_{obsd2} [s^{-1}]		
L-Met	288	280	1	4.11(4)	-	-	-
			2	7.81(5)	-	-	-
			3	11.49(5)	-	-	-
			4	15.86(4)	-	-	-
			5	19.52(6)	-	-	-
	298		1	6.07(5)	1.10(3)	-	-
			2	10.19(4)	1.92(2)	-	-
			3	15.13(5)	2.90(3)	-	-
			4	21.53(4)	3.90(3)	-	-
			5	26.67(6)	4.90(2)	-	-
	308		1	9.76(5)	-	-	-

			2	18.52(4)	-	-	-
			3	26.35(5)	-	-	-
			4	36.45(5)	-	-	-
			5	46.43(6)	-	-	-
Ligand	T [K]	λ [nm]	10^3 C_L [M]	k_{obsd1} [s^{-1}]	k_{obsd2} [s^{-1}]	10^3 k_{obsd3} [s^{-1}]	10^4 k_{obsd4} [s^{-1}]
L-Cys	288	280	1	2.07(5)	0.13(4)	-	-
			2	3.50(5)	0.23(5)	-	-
			3	5.15(6)	0.35(5)	-	-
			4	7.03(5)	0.47(5)	-	-
			5	9.27(6)	0.60(6)	-	-
	298		1	4.10(5)	0.16(4)	0.73(2)	0.51(2)
			2	6.74(5)	0.30(5)	1.20(2)	1.03(3)
			3	11.23(5)	0.47(5)	1.80(2)	1.35(2)
			4	13.81(6)	0.63(5)	2.50(3)	1.83(2)
			5	18.43(6)	0.76(5)	3.20(2)	2.51(3)
	308		1	4.45(4)	0.19(4)	-	-
			2	9.67(4)	0.35(5)	-	-
			3	13.55(5)	0.58(5)	-	-
			4	17.89(5)	0.76(5)	-	-
			5	22.94(6)	0.90(4)	-	-
Ligand	T [K]	λ [nm]	10^3 C_L [M]	k_{obsd1} [s^{-1}]	10^2 k_{obsd2} [s^{-1}]	10^3 k_{obsd3} [s^{-1}]	10^4 k_{obsd4} [s^{-1}]
L-His	288	280	1	1.12(4)	1.45(4)	-	-
			2	2.29(5)	2.67(5)	-	-
			3	3.29(4)	4.13(4)	-	-
			4	4.43(6)	5.55(5)	-	-
			5	5.59(5)	6.78(4)	-	-
	298		1	1.26(4)	3.20(4)	0.16(2)	0.25(2)
			2	2.41(5)	6.30(5)	0.34(2)	0.47(3)
			3	3.52(5)	9.70(5)	0.48(2)	0.69(2)
			4	4.80(4)	13.00(5)	0.65(3)	0.91(3)
			5	6.02(6)	15.80(5)	0.82(2)	1.20(3)
	308		1	2.24(4)	6.80(6)	-	-
			2	3.89(5)	13.30(5)	-	-

			3	5.97(5)	18.70(5)	-	-
			4	8.10(4)	26.50(5)	-	-
			5	10.26(4)	32.70(4)	-	-
Ligand	T [K]	λ [nm]	10^3 C_L [M]	k_{obsd1} [s^{-1}]	$10^3 k_{obsd2}$ [s^{-1}]		
5'-GMP	288	310	1	0.58(4)	-	-	-
			2	1.25(5)	-	-	-
			3	1.77(5)	-	-	-
			4	2.26(4)	-	-	-
			5	3.04(6)	-	-	-
	298		1	0.88(4)	0.08(3)	-	-
			2	1.66(5)	0.15(3)	-	-
			3	2.56(5)	0.24(2)	-	-
			4	3.47(5)	0.31(2)	-	-
			5	4.24(5)	0.38(3)	-	-
	308		1	1.44(4)	-	-	-
			2	2.96(5)	-	-	-
			3	4.55(5)	-	-	-
			4	6.04(5)	-	-	-
			5	7.33(4)	-	-	-

[a]Number of runs in parenthesis

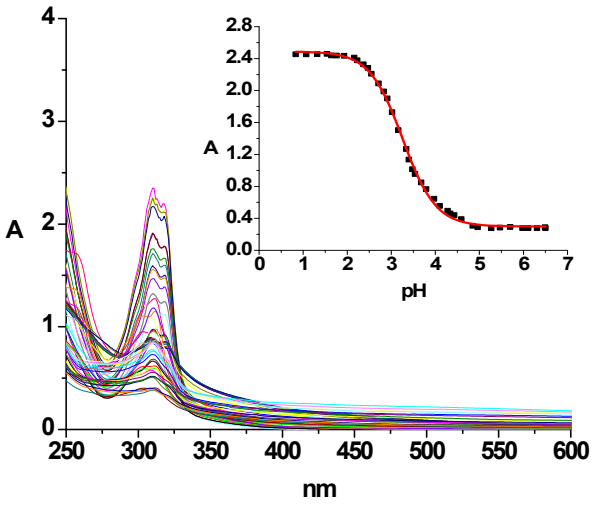

Fig. S1. Uv-Vis spectra of the diaqua $[\{Pd(H_2O)(en)\}\{\mu\text{-(pyrazine)}\}\{Pt(H_2O)(en)\}]^{4+}$ **(2a)** complex recorded as a function of pH in the pH range of 2 to 9 at I = 0.1 M $NaClO_4$ and 298 K. Insert graph: titration curve at 310 nm.

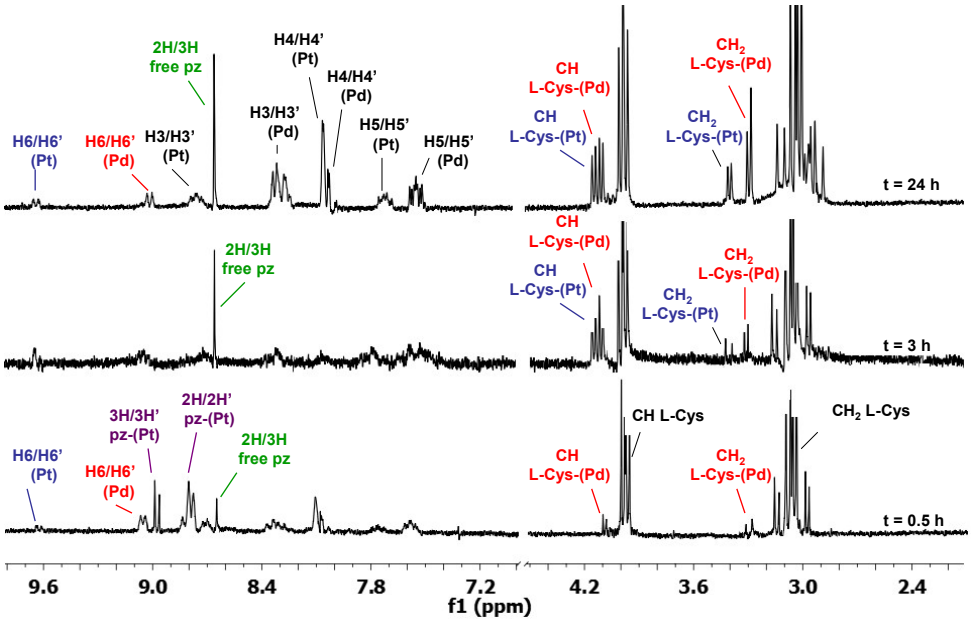

Fig. S2. ^{1}H NMR spectra of the complex **(1)** (2 mM) at various time intervals after the addition of L-Cys (8 mM, pH = 5.0, 295 K).

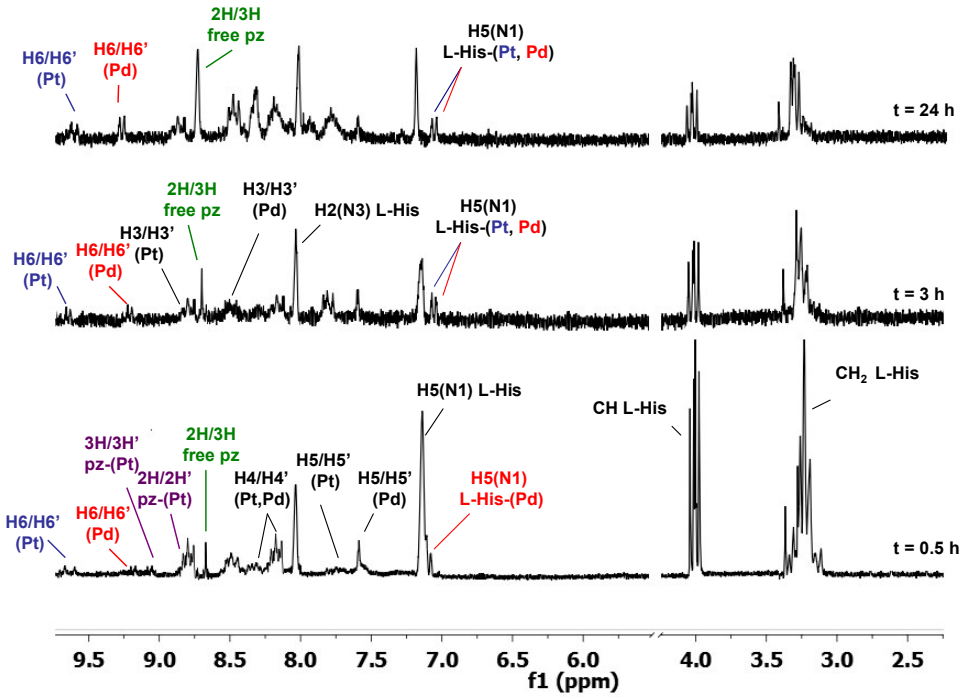

Fig. S3. ^{1}H NMR spectra of the complex **(1)** (2 mM) at various time intervals after the addition of L-His (8 mM, pH = 5.0, 295 K).

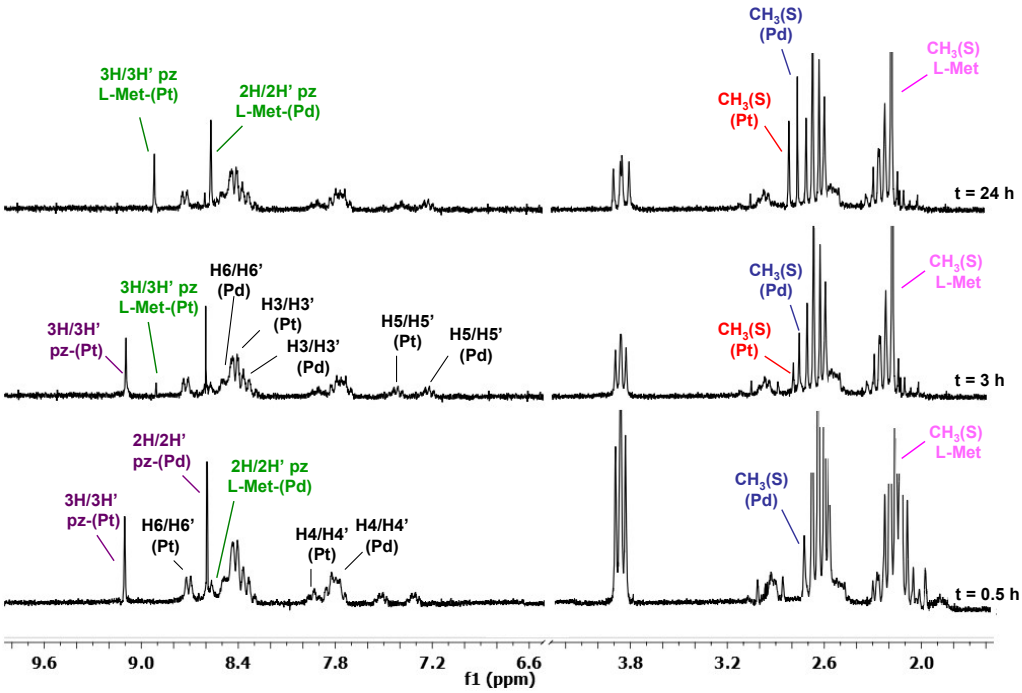

Fig. S4. ^{1}H NMR spectra of the complex **(1)** (2 mM) at various time intervals after the addition of L-Met (8 mM, pH = 5.0, 295 K).

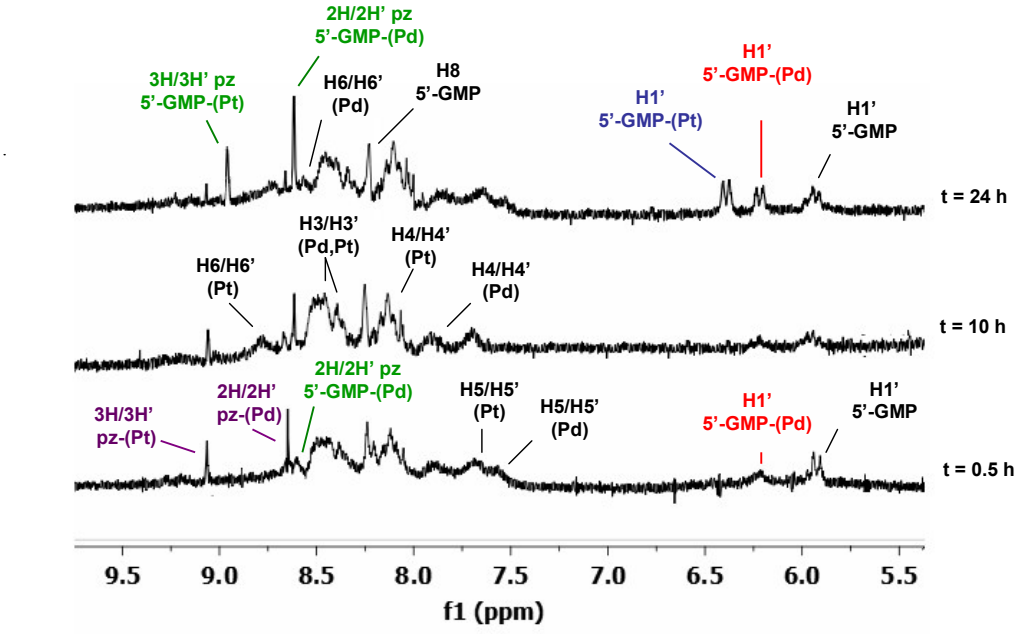

Fig. S5. ^{1}H NMR spectra of the complex **(1)** (2 mM) at various time intervals after the addition of 5'-GMP (8 mM, pH = 5.0, 295 K).

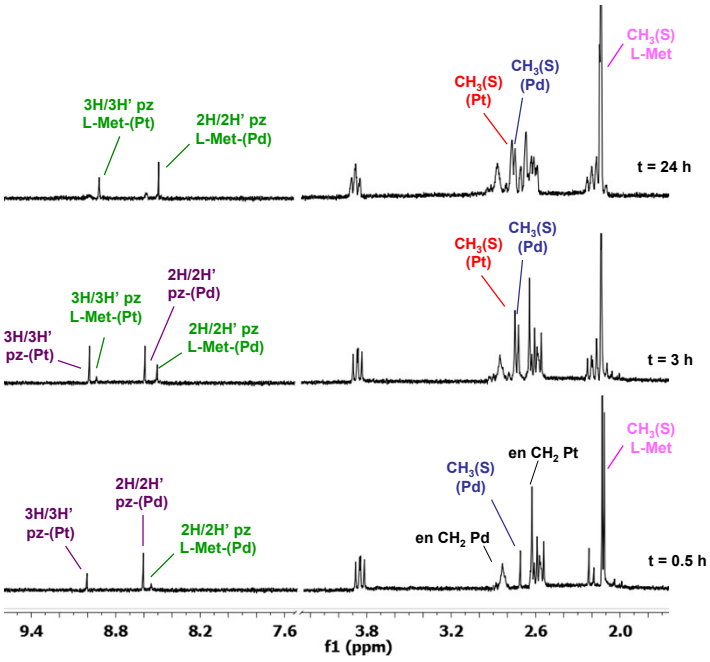

Fig. S6. ^{1}H NMR spectra of the complex **(2)** (2 mM) at various time intervals after the addition of L-Met (8 mM, pH = 5.0, 295 K).

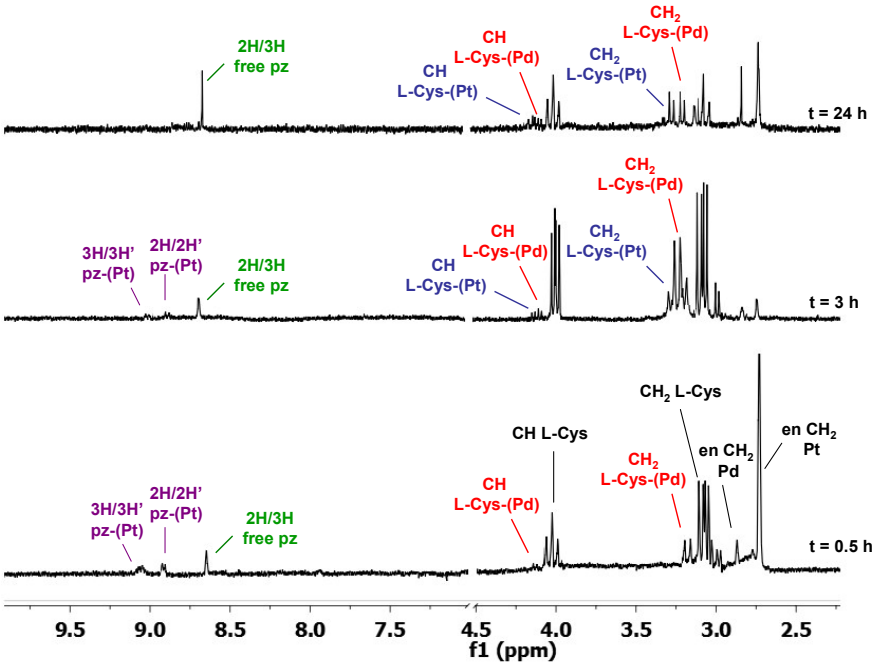

Fig. S7. ^{1}H NMR spectra of the complex **(2)** (2 mM) at various time intervals after the addition of L-Cys (8 mM, pH = 5.0, 295 K).

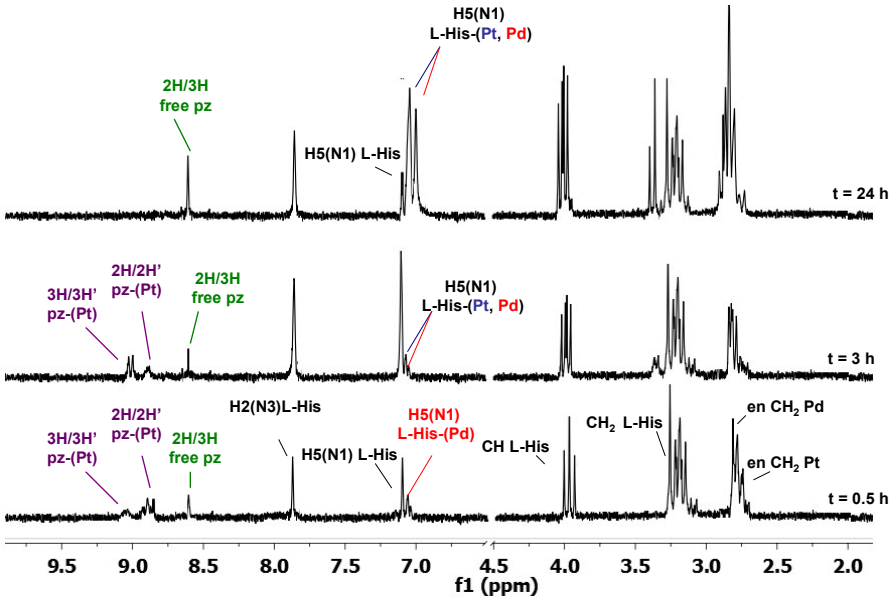

Fig. S8. ^{1}H NMR spectra of the complex **(2)** (2 mM) at various time intervals after the addition of L-His (8 mM, pH = 5.0, 295 K).

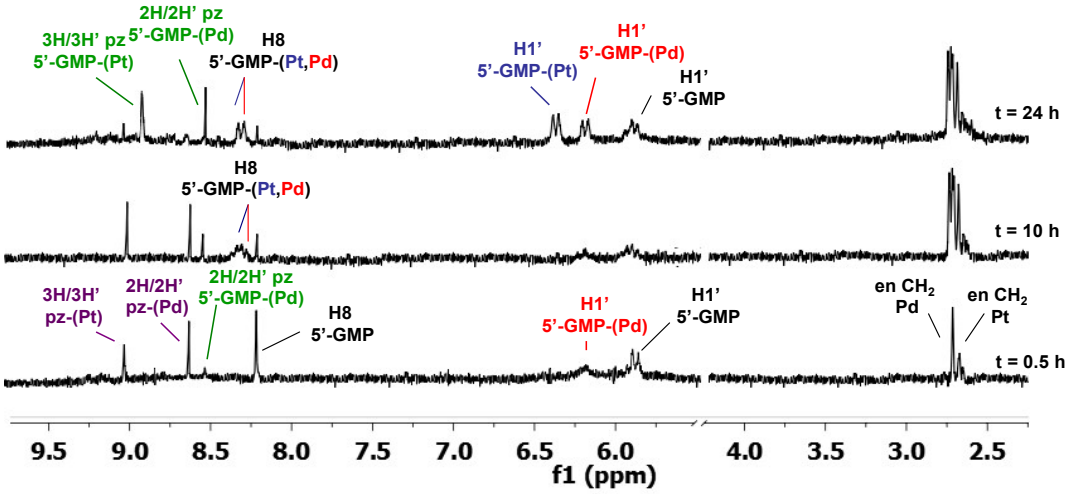

Fig. S9. ^{1}H NMR spectra of the complex **(2)** (2 mM) at various time intervals after the addition of 5'-GMP (8 mM, pH = 5.0, 295 K).

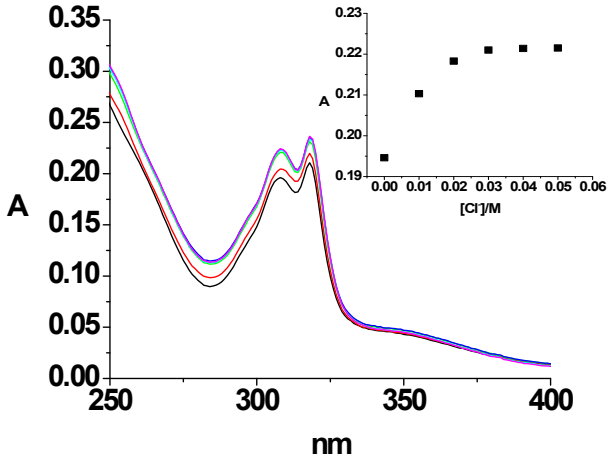

Fig. S10. Uv-Vis spectra of the complex **(1)** (10 mM) at pH 7.2 (25 mM Hepes buffer), recorded in the absence of NaCl (black line) and in the presence of the 10 mM NaCl (red line), 20 mM NaCl (green line), 30 mM NaCl (light blue line), 40 mM NaCl (blue line) and 50 mM NaCl (pink line). The dependence of the absorbance as a function of chloride concentration for the same reactions at 307 nm.

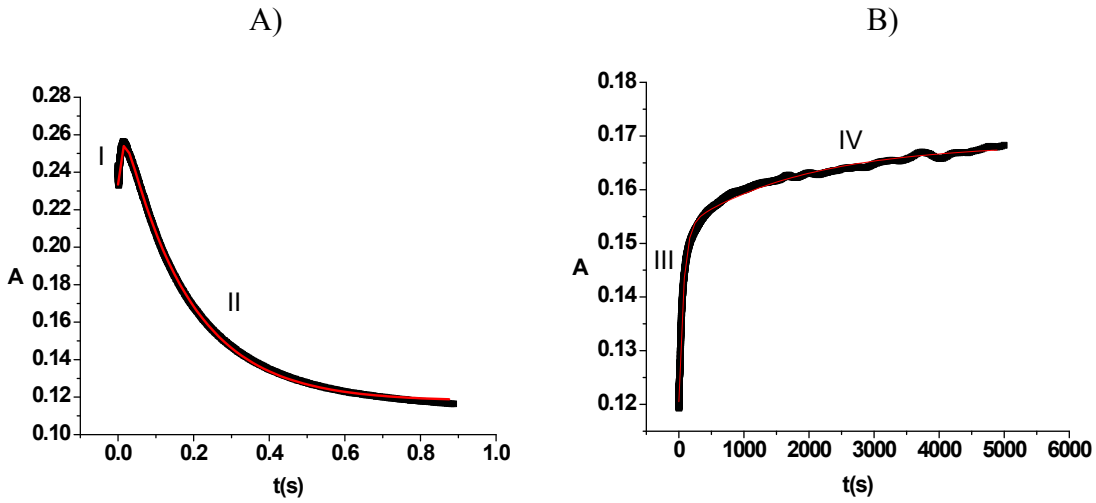

Fig. S11. Kinetic traces for the A) first (I) and the second (II) reaction steps and for the B) third (III) and fourth (IV) reaction steps of the substitution reaction between complex **(1)** (0.1 mM) and Tu (1 mM) at 298 K (310 nm) in 25 mM Hepes buffer (pH = 7.2) with addition 40 mM NaCl.

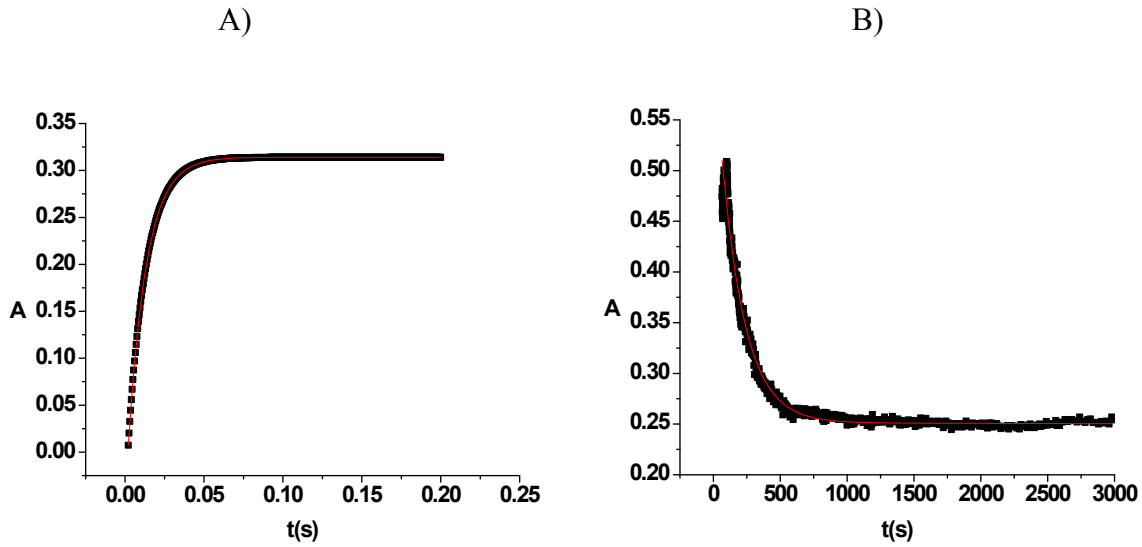

Fig. S12. Kinetic traces for the first (A) and for the second (B) reaction steps of the substitution reaction between complex **(2)** (0.1 mM) and L-Met (3 mM) at 298 K (280 nm) in 25 mM Hepes buffer (pH = 7.2) with the addition of 40 mM NaCl.

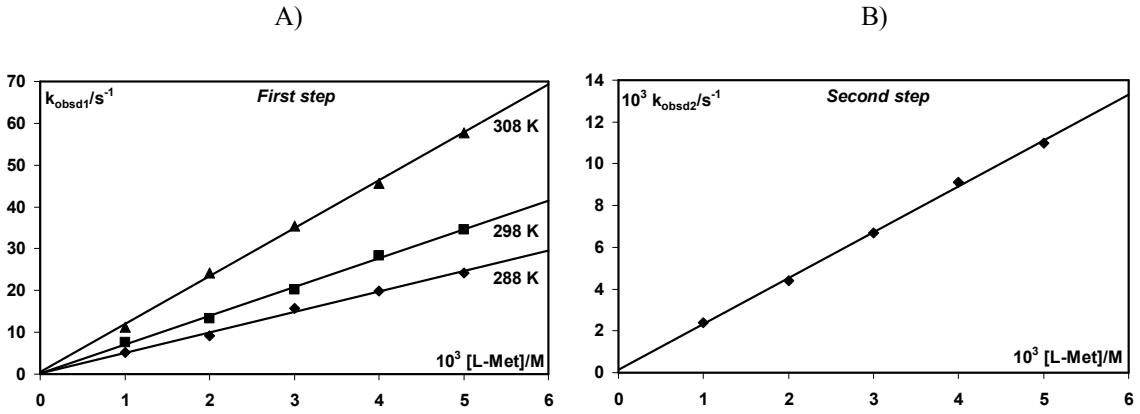

Fig. S13. *Pseudo*-first order rate constants plotted as a function of nucleophile concentration for the first (A) substitution step at 288 K 298 K, 308 K and for the second (B) reaction step at 298 K for the substitution reactions of complex **(1)** with L-Met at pH = 7.2 (25 mM Hepes buffer) with the addition of 40 mM NaCl.

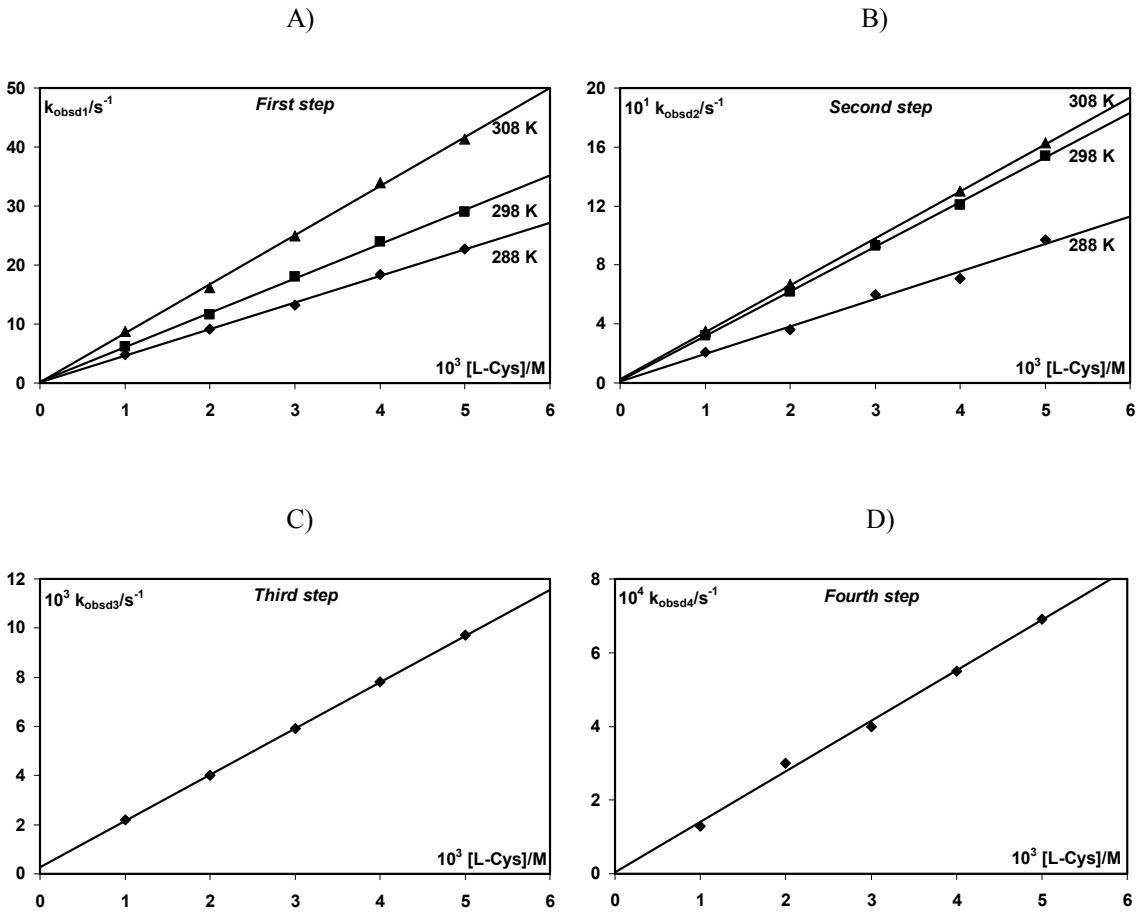

Fig. S14. *Pseudo*-first order rate constants plotted as a function of nucleophile concentration for the first (A) and second (B) reaction steps at 288 K, 298 K and 308 K, and for the third (C) and fourth (D) reaction steps at 298 K for the substitution reactions of complex **(1)** with L-Cys at pH = 7.2 (25 mM Hepes buffer) with the addition of 40 mM NaCl.

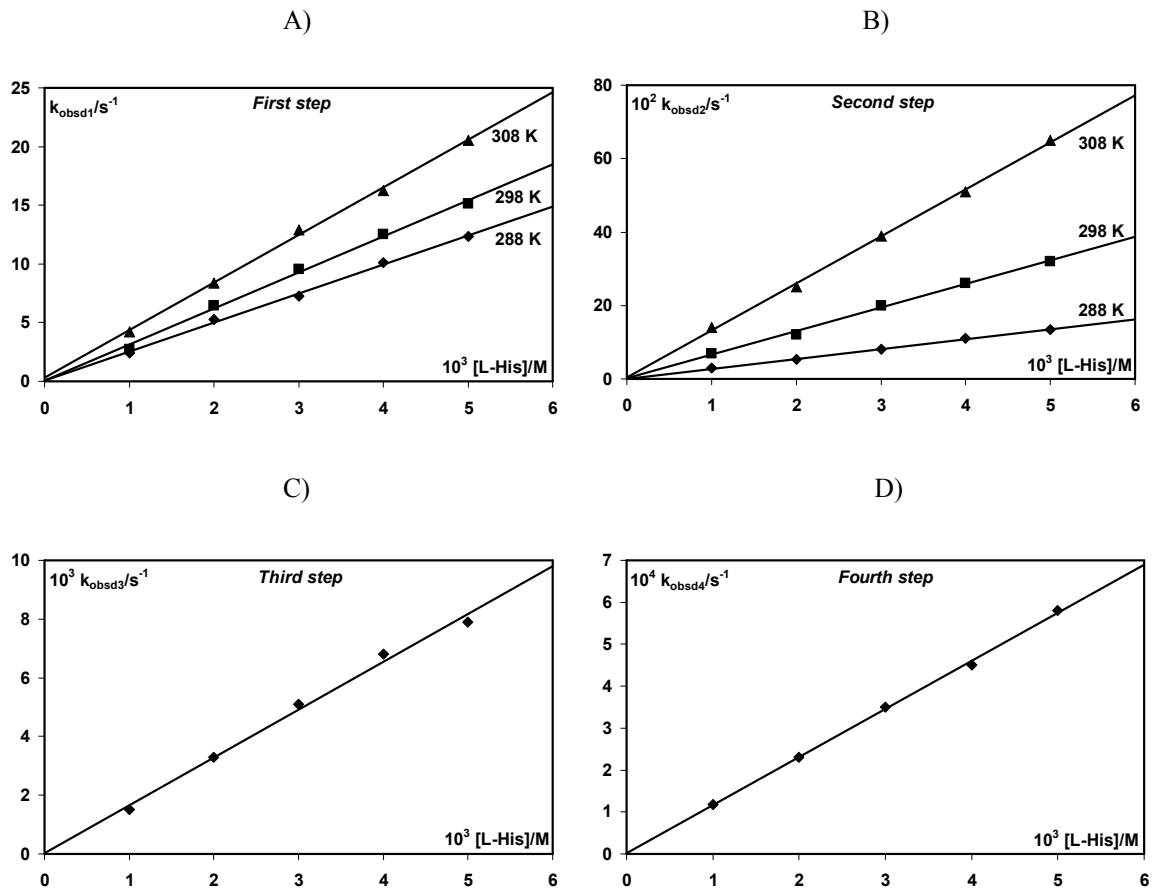

Fig. S15. *Pseudo*-first order rate constants plotted as a function of nucleophile concentration for the first (A) and second (B) reaction steps at 288 K, 298 K and 308 K, and for the third (C) and fourth (D) reaction steps at 298 K for the substitution reactions of complex **(1)** with L-His at pH = 7.2 (25 mM Hepes buffer) with the addition of 40 mM NaCl.

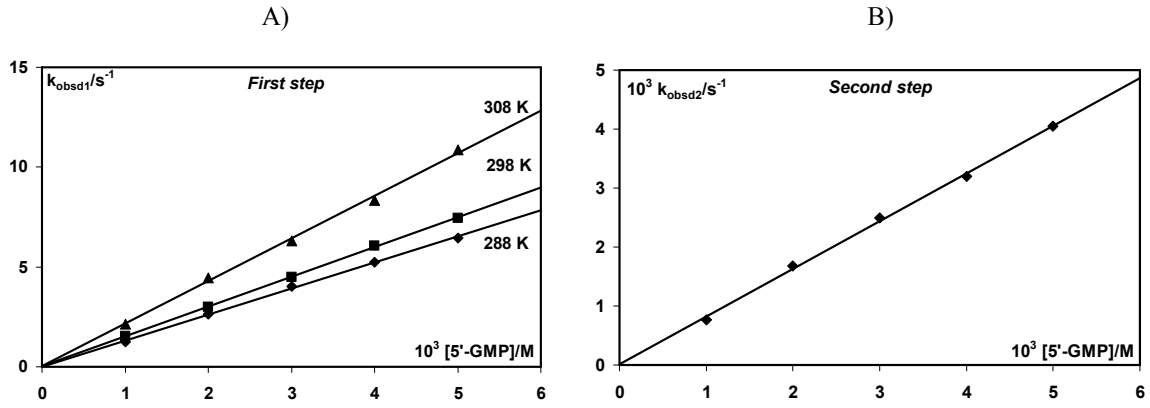

Fig. S16. *Pseudo*-first order rate constants plotted as a function of nucleophile concentration for the first (A) substitution step at 288 K 298 K, 308 K and for the second (B) reaction step at 298 K for the substitution reactions of complex **(1)** with 5'-GMP at pH = 7.2 (25 mM Hepes buffer) with the addition of 40 mM NaCl.

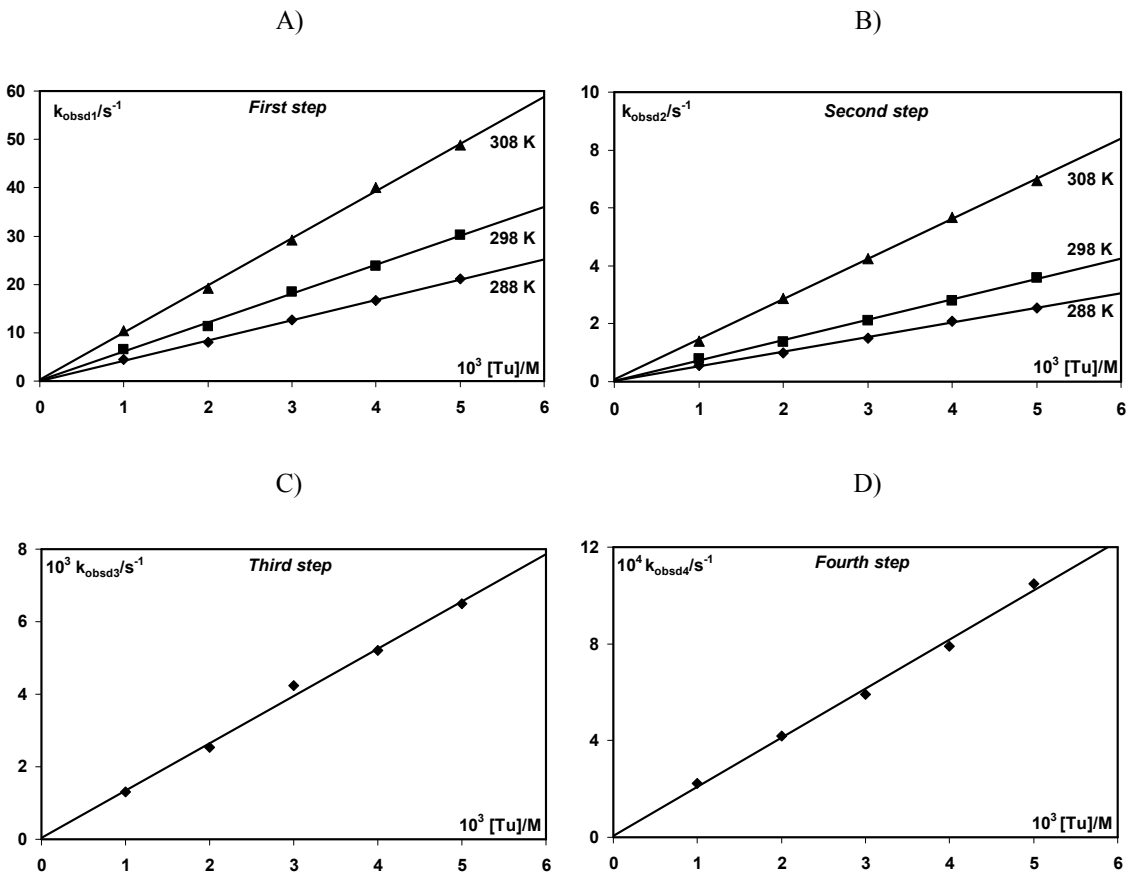

Fig. S17. *Pseudo*-first order rate constants plotted as a function of nucleophile concentration for the first (A) and second (B) reaction steps at 288 K, 298 K and 308 K, and for the third (C) and fourth (D) reaction steps at 298 K for the substitution reactions of complex **(2)** with Tu at pH = 7.2 (25 mM Hepes buffer) with the addition of 40 mM NaCl.

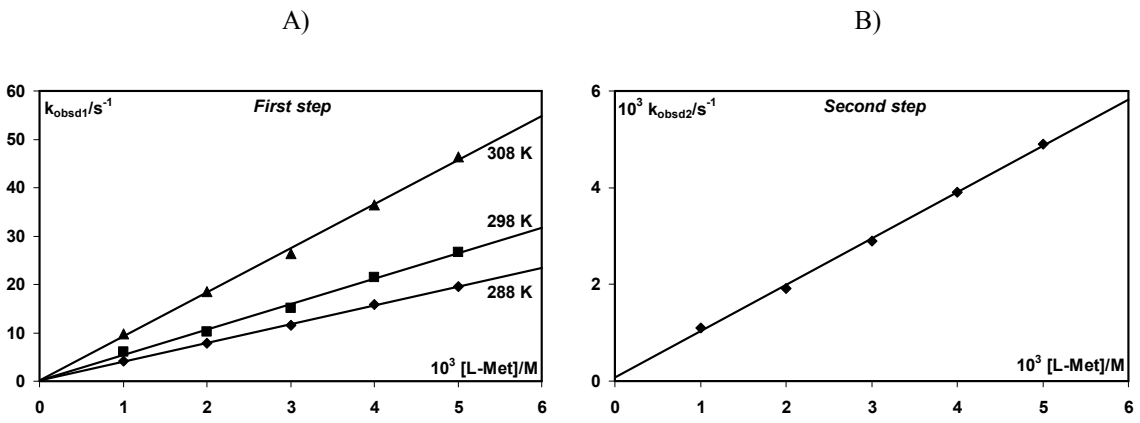

Fig. S18. *Pseudo*-first order rate constants plotted as a function of nucleophile concentration for the first (A) substitution step at 288 K 298 K, 308 K and for the second (B) reaction step at 298 K for the substitution reactions of complex **(2)** with L-Met at pH = 7.2 (25 mM Hepes buffer) with the addition of 40 mM NaCl.

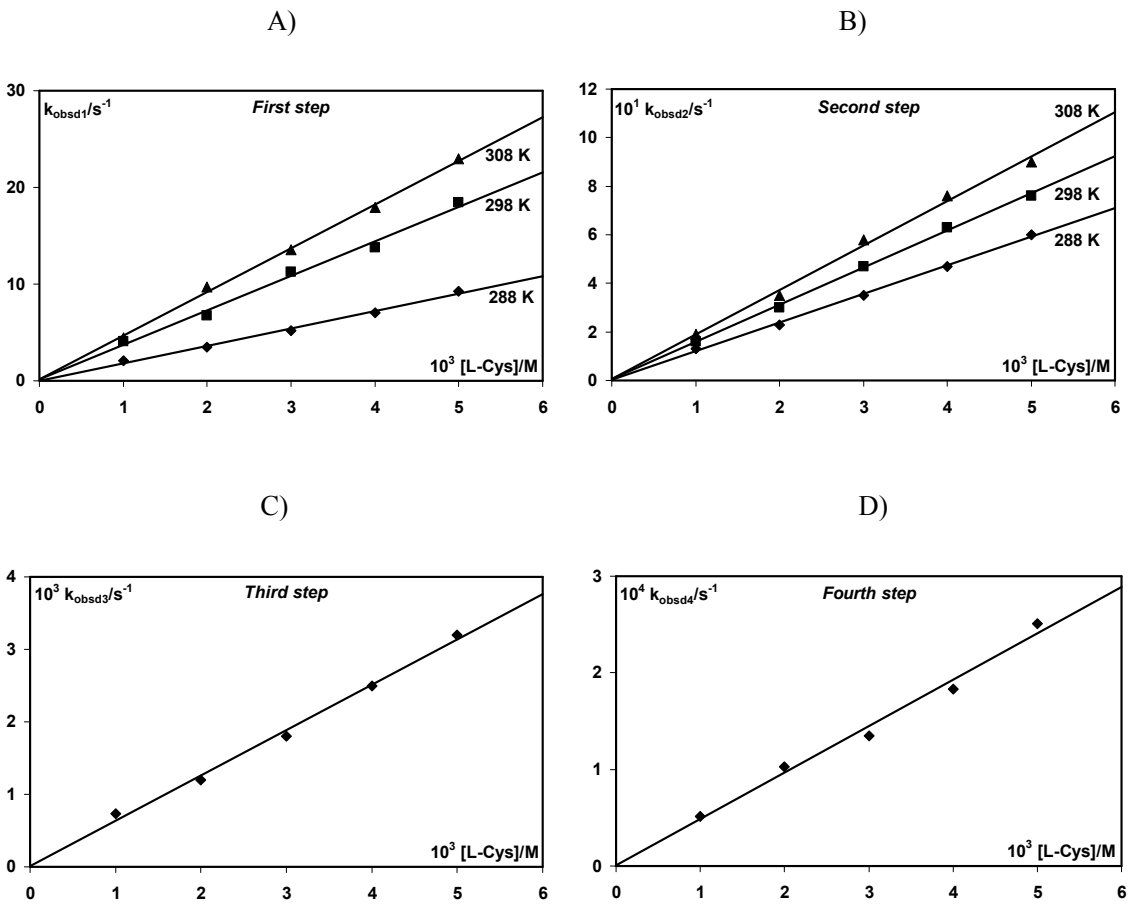

Fig. S19. *Pseudo*-first order rate constants plotted as a function of nucleophile concentration for the first (A) and second (B) reaction steps at 288 K, 298 K and 308 K, and for the third (C) and fourth (D) reaction steps at 298 K for the substitution reactions of complex **(2)** with L-Cys at pH = 7.2 (25 mM Hepes buffer) with the addition of 40 mM NaCl.

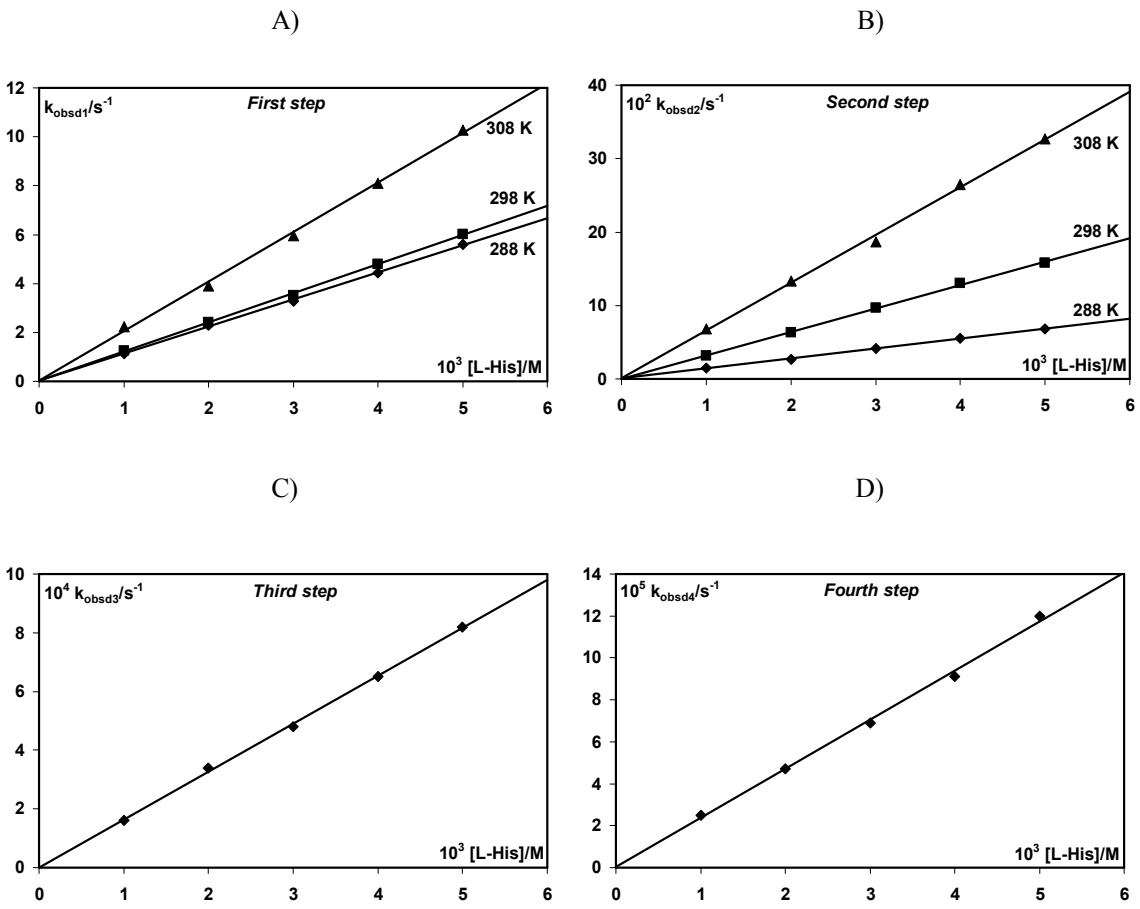

Fig. S20. *Pseudo*-first order rate constants plotted as a function of nucleophile concentration for the first (A) and second (B) reaction steps at 288 K, 298 K and 308 K, and for the third (C) and fourth (D) reaction steps at 298 K for the substitution reactions of complex **(2)** with L-His at pH = 7.2 (25 mM Hepes buffer) with the addition of 40 mM NaCl.

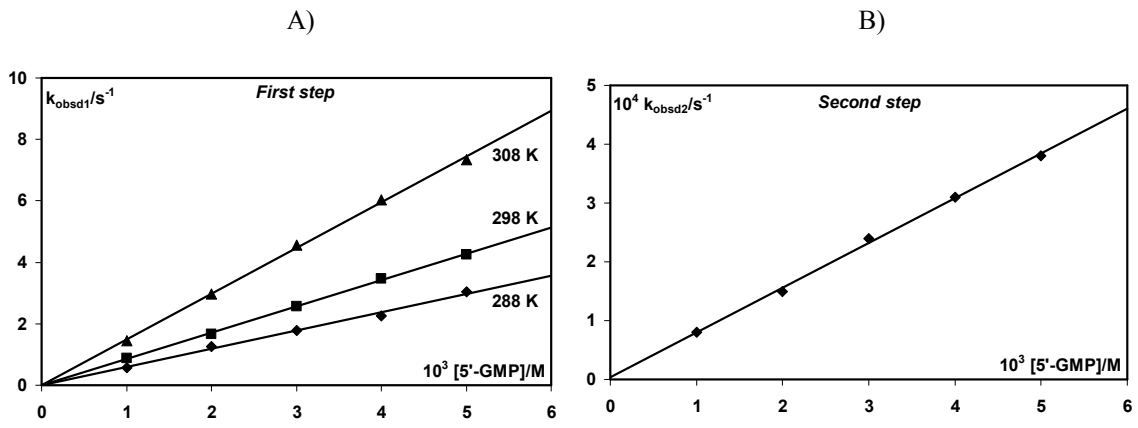

Fig. S21. *Pseudo*-first order rate constants plotted as a function of nucleophile concentration for the first (A) substitution step at 288 K 298 K, 308 K and for the second (B) reaction step at 298 K for the substitution reactions of complex **(2)** with 5'-GMP at pH = 7.2 (25 mM Hepes buffer) with the addition of 40 mM NaCl.

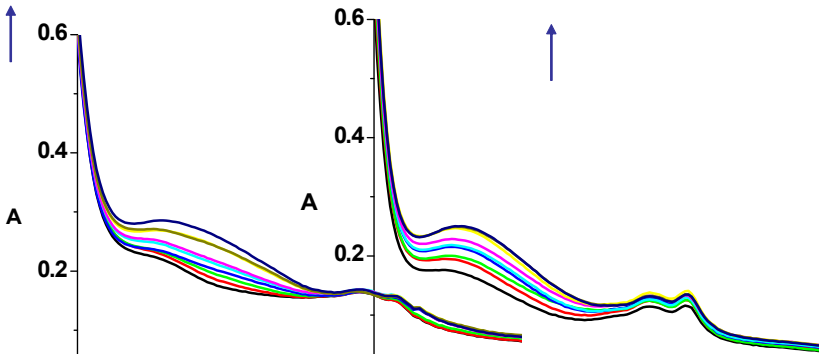

Fig. S22. Absorption spectra of the complexes **(1)** (left) and **(3)** (right) in PBS buffer upon addition of calf thymus DNA. [complex] = 8 x 10^{-6} M, [DNA] = (0-12.8) x 10^{-6} M. Arrow shows the absorbance changing upon increasing DNA concentrations.

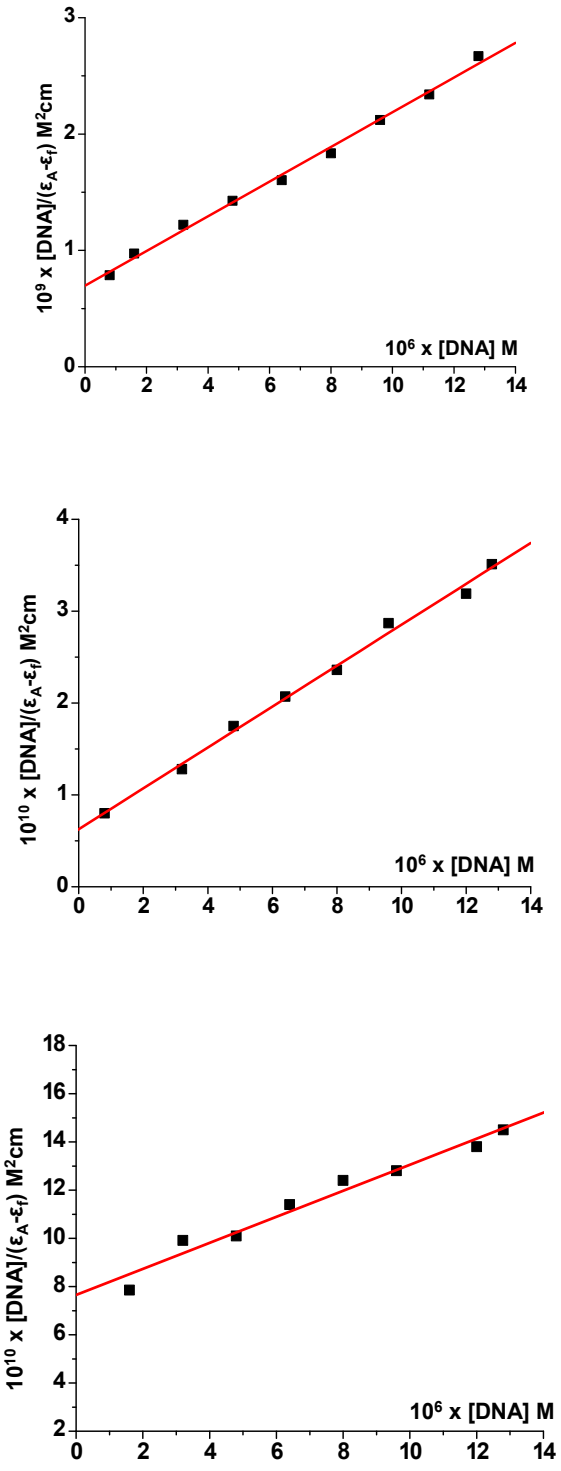

Fig. S23. Plot of [DNA]/($\varepsilon_A - \varepsilon_f$) vs. [DNA] for the complexes **(1)** (top), **(2)** (middle) and **(3)** (bottom).

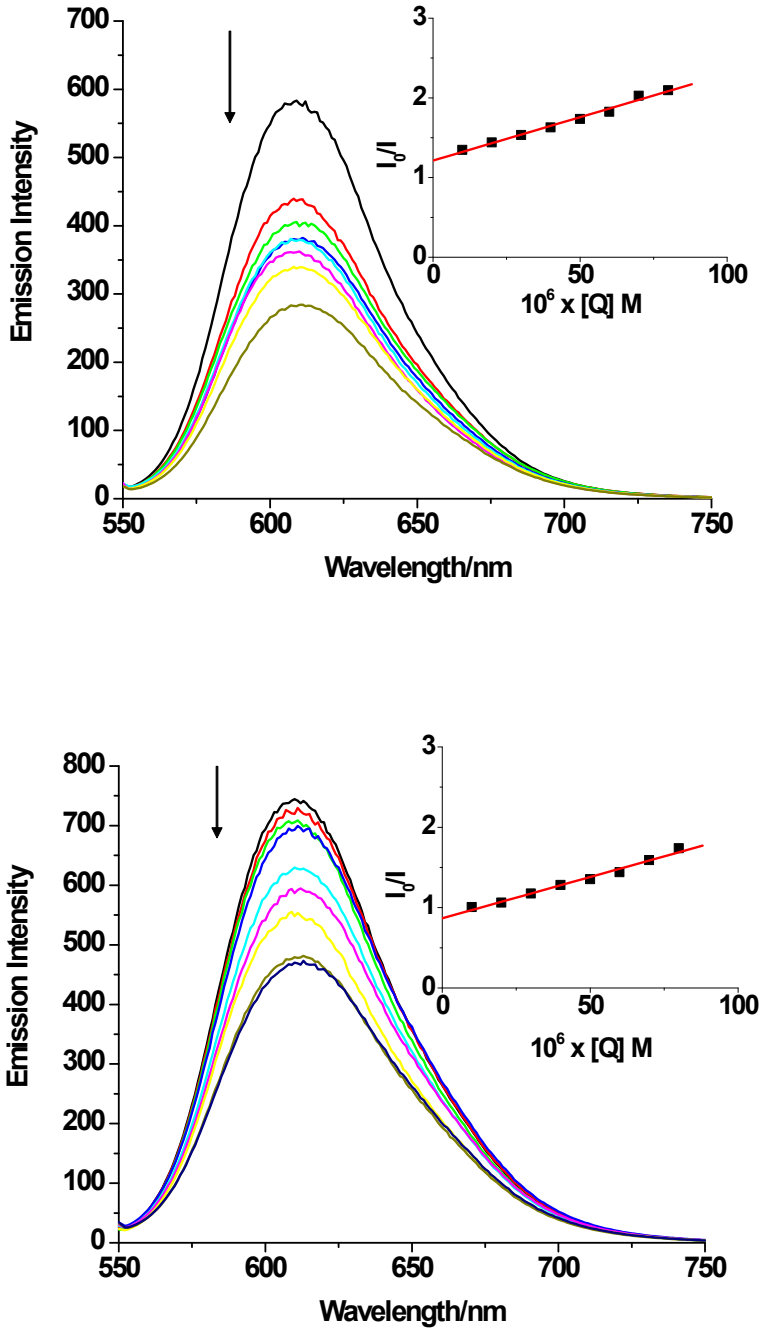

Fig. S24. Emission spectra of EB bound to DNA in the presence of complexes **(2)** (top) and **(3)** (bottom). [EB] = 50 μM, [DNA] = 50 μM; [complex] = 0-80 μM; λ_{ex} = 527 nm. The arrows show the intensity changes upon increasing concentrations of the complexes. Insets: plots of I_0/I *vs.* [Q], with ■ for the experimental data points and the full line for the linear fitting of the data.

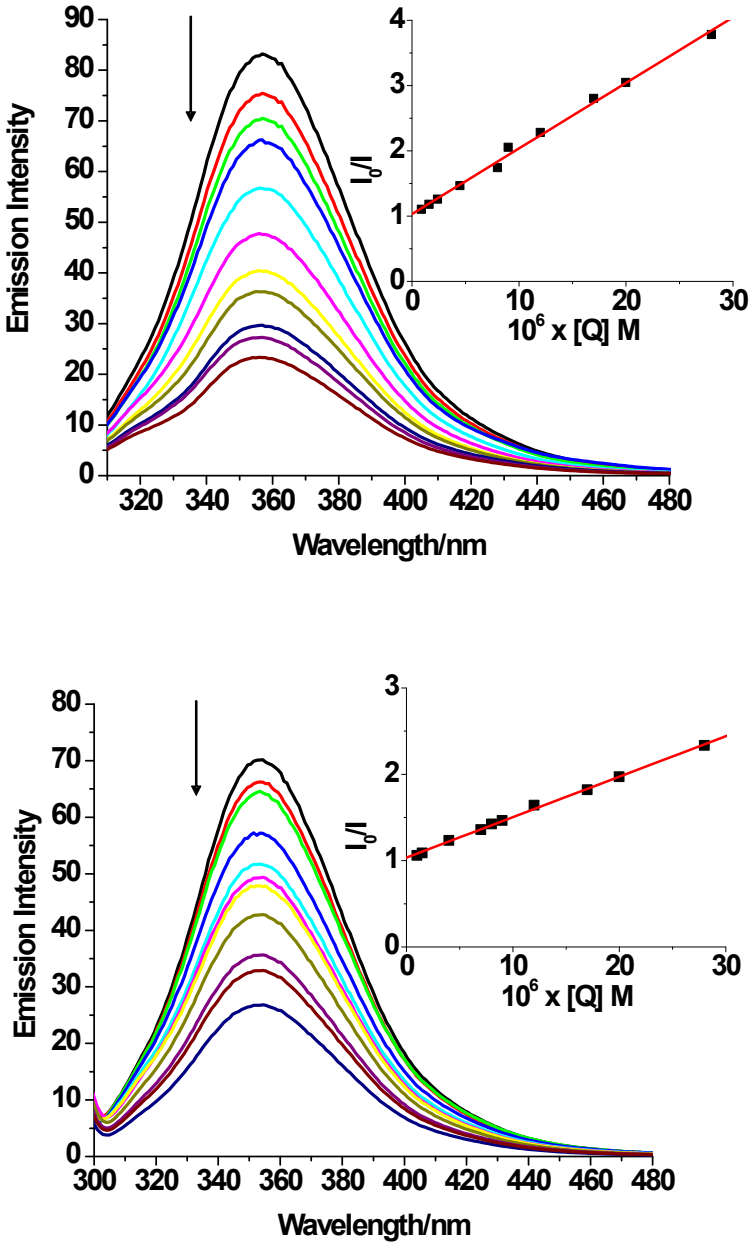

Fig. S25. Emission spectra of BSA in the presence of complexes **(2)** (top) and **(3)** (bottom). [BSA] = 2 μM, [complex] = 0-28 μM; λ_{ex} = 295 nm. The arrows show the intensity changes upon increasing concentrations of the complex. Inset: plots of I_0/I *versus* [Q], with ■ for the experimental data points and the full line for the linear fitting of the data.

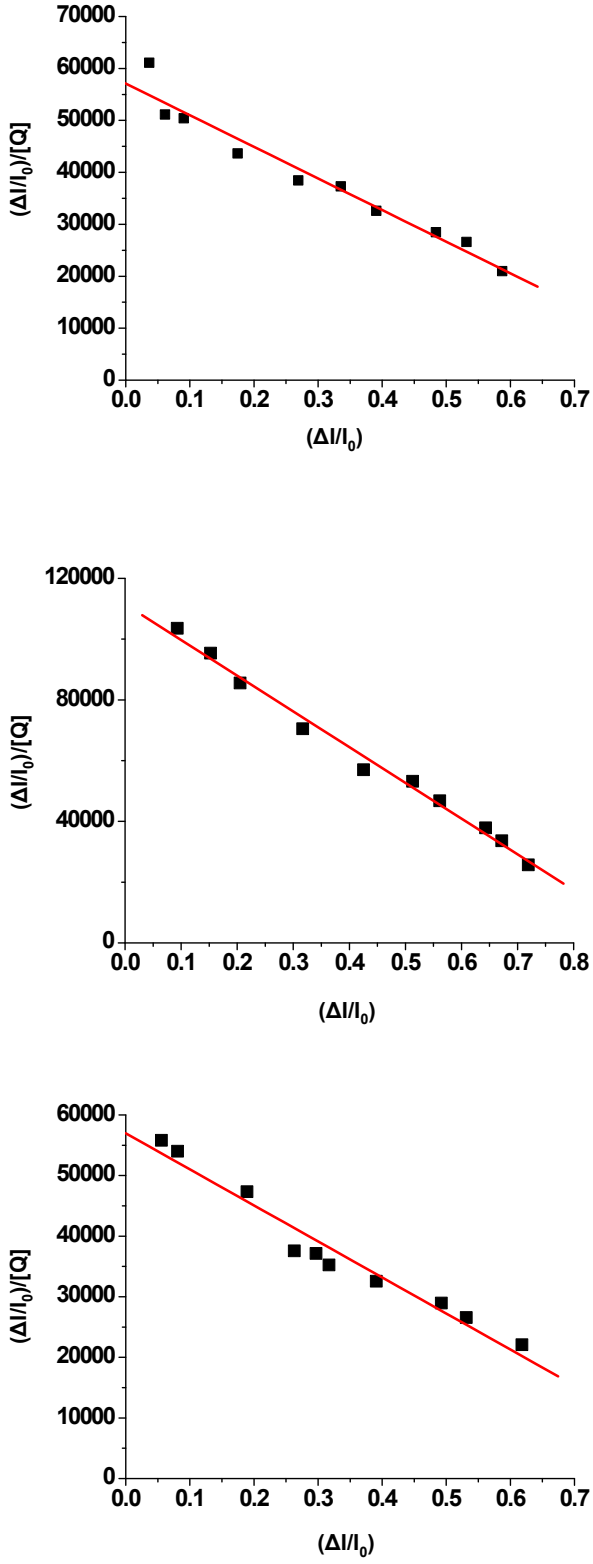

Fig. S26. Scatchard plots of BSA for complexes **(1)** (top), **(2)** (middle) and **(3)** (bottom).

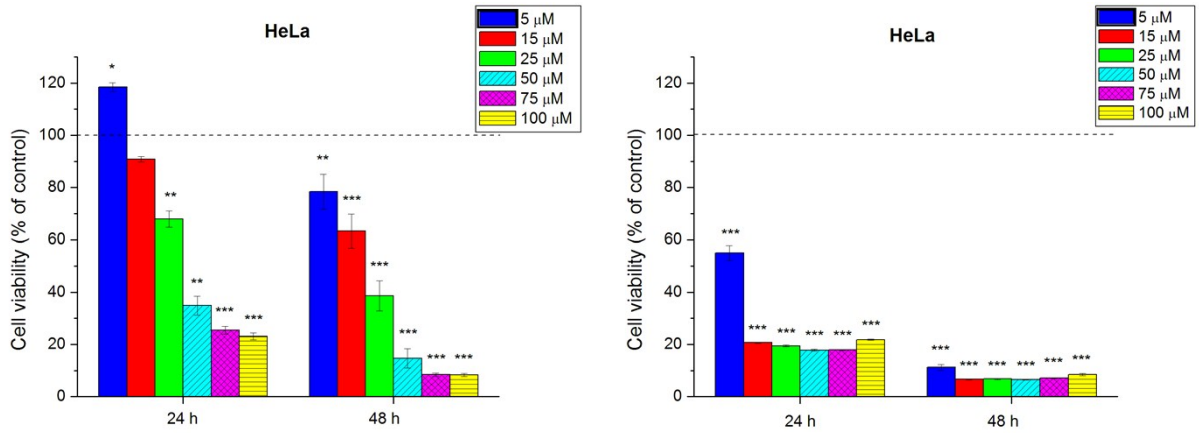

Fig. S27. Viability of HeLa cells exposed to treatment with complex **(1)** (left) and cisplatin (right) (5-100 μM) for 24 and 48 h. Data are presented as means ± S.D. * - Statistical significance compared to the control; * - 0.01 < p < 0.05; ** - 0.001 < p < 0.01; *** - p < 0.001.

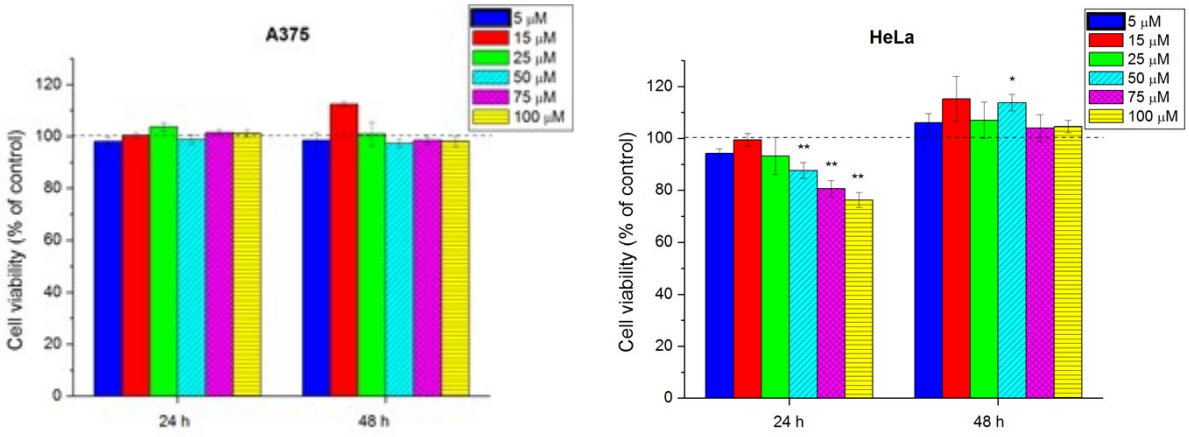

Fig. S28. Viability of A 375 cell (left) and HeLa cell (right) exposed to treatment with complex **(2)** (5-100 μM) for 24 and 48 h. Data are presented as means ± S.D. * - Statistical significance compared to the control; * - 0.01 < p < 0.05; ** - 0.001 < p < 0.01; *** - p < 0.001.

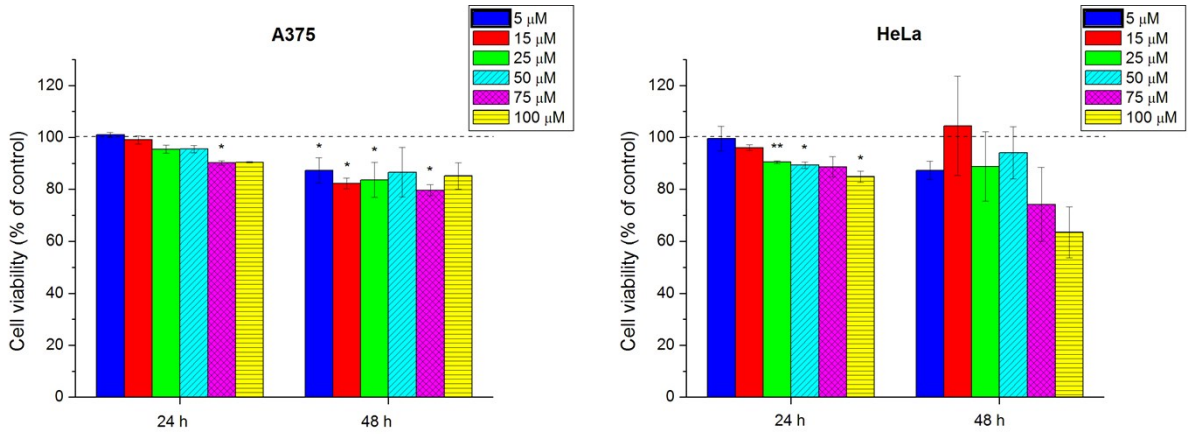

Fig. S29. Viability of A 375 cell (left) and HeLa cell (right) exposed to treatment with complex **(3)** (5-100 μM) for 24 and 48 h. Data are presented as means ± S.D. * - Statistical significance compared to the control; * - $0.01 < p < 0.05$; ** - $0.001 < p < 0.01$; *** - $p < 0.001$.

a) Complex (1)

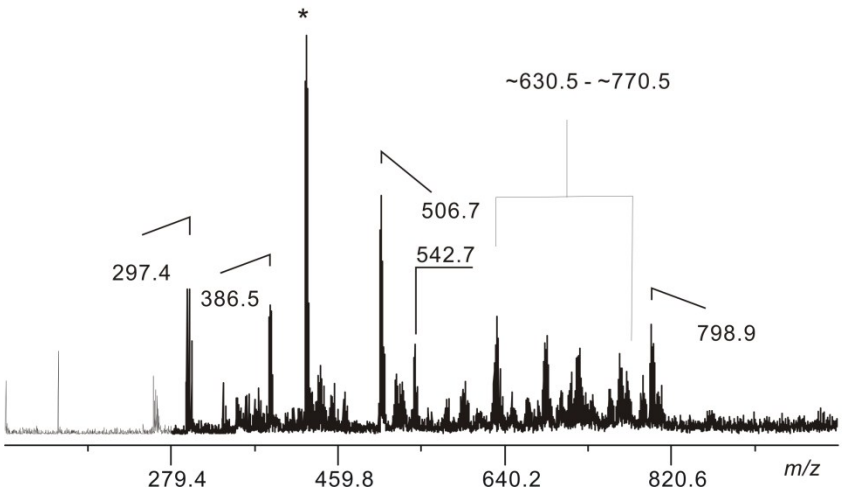

b) Complex (2)

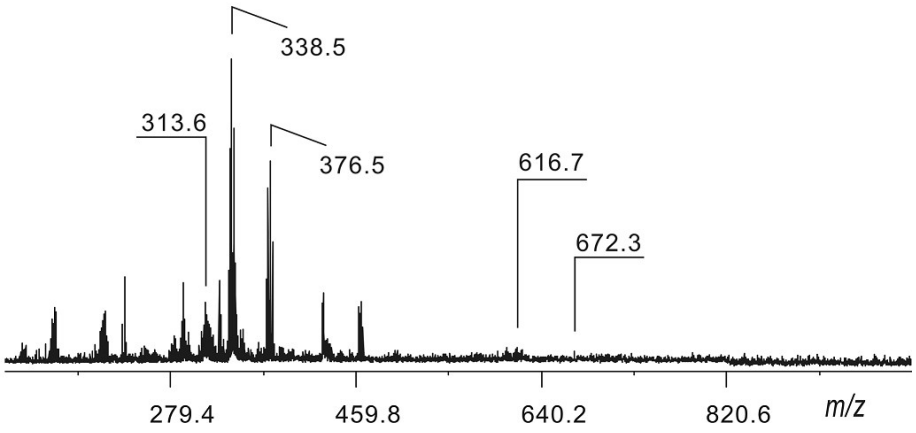

Fig. S30 Positive ion MALDI-TOF mass spectra of the a) complex **(1)** and b) complex **(2)**. Signals are indicated according to their position and their identity is given in Table S1. Spectrum is acquired under delayed extraction condition and in the reflector mode to increase accuracy and resolution.